International Journal Of
Industrial Electronics Control and Optimization
Print ISSN: 3517-2645
Online ISSN: 3568-2645
Homepage: https://ieco.usb.ac.ir/

Transformer Winding-to-Ground Connection Internal Fault Locating using the Estimation Error Standard Deviation Index

Mohammad Ali Taghikhani
Department of Engineering, Imam Khomeini International University, Qazvin, Iran
Corresponding Author Email: taghikhani@eng.ikiu.ac.ir

Article Info

Article type:
Research Article

Article history:
Received: **********
Received in revised form: **********
Accepted: **********
Published online: **********

Keywords:
Estimation,
Extended Kalman filter (EKF),
Fault location,
Inrush current,
Standard deviation

ABSTRACT

Protective relay in the transformer may accept inrush current as fault current, thus, distinguishing the inrush current from the internal fault current is important in transformers. To estimate the transformer inrush current, the extended Kalman filter (EKF) is applied in this paper. Therefore, three phase transformer initial inrush currents are estimated using the extended Kalman filter formulation and a nonlinear model is used to simulate inrush currents. Then, type of current, whether it is a fault or an inrush current, is determined by comparing this current and the current calculated from the transformer model. It is considered as a fault current, if the inrush current estimation error surpasses a certain limit compared to the transformer actual inrush current. On the other hand, connection of the winding to the ground fault location has been also presented in this paper which has been less investigated in previous studies. Also, the relation of the fault location to the estimation error standard deviation is also studied and an index β is introduced. If the value of this index is greater than a specific value in any phase of the transformer, a fault condition is identified. Finally, the proposed technique is implemented for another transformer to calculate the estimation error standard deviation and index β in the faulty condition. The results show the index β values are in agreement with the index limits and validate the accuracy of the proposed method.

NOMENCLATURE

f	Frequency: Hz	r	The transformer winding resistance: Ω
i_ψ	The magnetizing current: A	r_{mag}	The magnetizing branch resistance: Ω
i_{inr}	The inrush current: A	v_s	Source voltage: V
l	The transformer winding self-inductance: H	α	Switching angle:°
m	The transformer winding mutual inductance: H	ψ	Core flux-turn: Wb.t

I. Introduction

One of the most important protections which is used for power transformers is differential protection [1]. In transient conditions, while the transformer is initially connected to the voltage source, an inrush current is generated, in which the relay should not work. In these conditions, harmonic inhibition methods usually are used to stabilize the relay against the transformer inrush current. But in transformers with better quality cores, the amount of second and fifth harmonics are low, so their detection may be done with error. To solve this problem, studies have been carried out to detect the transformer inrush current in the past years. The frequency domain reflectometry (FDR) technique for detecting and locating transformer winding defects has been proposed in [2]. FDR measures the wave impedance and its change along the measured windings. In some methods, considering that the inrush current has only an active power close to zero, but in the fault mode active power is consumed, the transformer input power is checked to discriminate the inrush current from the internal fault current. The important disadvantage of this method is its slow response time, which is more than one cycle. The current variation characteristics of inter-turn short-circuit faults in grounding transformers under various operating conditions has been presented in [3] through theoretical analysis, simulations, and case studies. An online identification method is proposed in [3] to detect inter-turn short-circuit faults in grounding transformer windings and to distinguish affected phases based on current variation characteristics.

Some researchers have proposed artificial intelligence methods, including fuzzy methods and neural networks for high speed distinguishing the transformer inrush current

from the internal fault current. Although these methods increase the speed and bring it below one cycle, but those are among learning-based methods and require large datasets [4]. In [5], a fault diagnosis method is presented for identifying multi-point grounding faults in transformer cores based on the finite element method (FEM). On the other hand, the internal temperature distribution within the transformer and the condition of the transformer oil are comprehensively analyzed and validated by using an electromagnetic-fluid-solid coupled finite element simulation. It is important to mention that the fault occurrence in a point of the transformer winding causes the hot spot creation and ultimately leads to the insulation destruction. A new transformer fault diagnosis method has been investigated in [6] based on the parallel AdaBoost-Naive Bayes algorithm. This method allows for resampling and reweighting, making the model pay more attention to samples that are difficult to classify and thereby improving performance on imbalanced datasets. Frequency response analysis (FRA) is one of the winding fault detection methods and the FRA is offline which it is a negative feature [7].

In [8] finite element method has been used for fault location in the transformer. In this paper force measuring sensors have been also placed in parts of the transformer windings to measure the forces applied to the windings during short circuit as online. The most disadvantages of the method in [8] are due to placing the sensor and additional winding in the transformer. Therefore, the flux-based technique is introduced in [9] to determine the location of the fault in the winding and is used to solve the problems in [8]. Among the other methods in fault location are artificial intelligence based methods. But these methods, in spite of many advantages, require a lot of dataset and system initial training [10]. The wavelet transform method and artificial intelligence are used in [11] to show the location of the fault in the transformer winding-to-ground connection. A time-domain analytical–numerical method has been proposed in [12] for inrush current modeling in three-phase core-type transformers, incorporating the nonlinear magnetic behavior of the core. A novel algorithm for transformer differential protection is proposed in [13] which distinguishes internal faults from inrush currents in the presence of CT saturation. To reduce the effect of CT saturation, the currents are compensated by a CT saturation compensation method. Then, wavelet transform is used to discriminate transformer internal fault from inrush currents. In [14] a differential protection method is suggested, which decomposes the differential current signal to multiple energy levels through the multi-resolution analysis (MRA) and selects the most useful feature to feed to the bidirectional gated recurrent unit (BIGRU) to classify the events.

To differentiate the transformer's internal fault from the inrush current, convolutional neural network (CNN) is used in [15]. Therefore, a combination of the higher order spectral estimations that perform a deep learning classification with high accuracy, are proposed. In this paper, the extended Kalman filter has been used to distinguish between inrush current and fault current in the transformer winding as well as to show the location of the winding fault. The EKF does not have the disadvantages of the above mentioned methods. This filter has the online nature, low computational rate, and the elimination (or maximum reduction) of process and measurement noises [16]. The nonlinear model of a single-phase transformer is derived in [17] which includes the hysteresis and magnetic saturation, and then an EKF is used for estimation of the primary winding current to distinguish the transformer inrush current from an internal fault current.

A statistical algorithm for discrimination of fault and inrush current signals under CT saturation scenarios is proposed in [18] and twofold discrimination indices centered on the concept of fourth-order statistic moment are presented. A method is suggested in [19] to distinguish the internal fault of transformers and other normal transient conditions, and operational characteristic is defined for classification of the instantaneous current behavior based on the modal transform. The Hermite transform method is considered in [20] to identify transient events in power transformers caused by energizations and current transformer (CT) saturation. In this approach, the positive half-cycle is analyzed firstly and then negative half-cycle is studied. A sensitive method based on wavelet transform for detecting inter-turn faults during energization of single-distribution transformers under healthy and faulty conditions is suggested in [21]. The waveform features are obtained by the mathematical morphology gradient (MMG) operator in [22] and then the morphological pattern spectrum (MPS) is applied to discriminate between inrush current and fault current. A transformer differential protection algorithm is presented in [23] so that between inter-turn, low-level internal faults, and inrush current is differentiated. Feature is extracted using difference function and maximum overlapped discrete wavelet transform energy in this method. In [24] digital image processing method on a new FRA signature is used, so that the frequency, magnitude, and phase angle of the conventional FRA signature are integrated into one 3D plot to classify various faults. The measurement process overview of fault detection and location in power transformers using frequency response analysis is proposed in [25].The use of the EKF method to estimate the single-phase transformer inrush current have been investigated in various references, but based on the authors' best knowledge, the extended Kalman filter has not been developed for fault location in three-phase transformer. Therefore, in the present paper, to discriminate inrush current from fault current without complex calculations, an algorithm has been developed. On the other hand, a method has been proposed

and formulated to show location of the winding fault using variance of the Kalman filter estimation error. The paper is arranged as follows: Section II describes three phase transformer inrush current modeling. Extended Kalman filter and inrush current simulation results are proposed in section III. Fault current simulation is investigated in section IV. Discriminating the fault from the inrush current, the winding fault location and verification of the accuracy of the proposed technique are studied in section V. Lastly, conclusion is brought in section VI.

II. Three Phase Transformer Inrush Current Modeling

A suitable model of the transformer is necessary to use the Kalman filter. Therefore, transformer nonlinear model is considered in this paper. On the other hand, for this purpose, nonlinear Kalman filter such as the extended Kalman filter should be developed. The nonlinearities of the transformer core have the greatest impact in the transformer inrush current modeling. Due to the low frequency of the inrush current phenomenon, there is no need to enter the transformer parameters frequency dependence into the modeling [26]. Figure 1 shows a three-phase transformer electrical circuit.

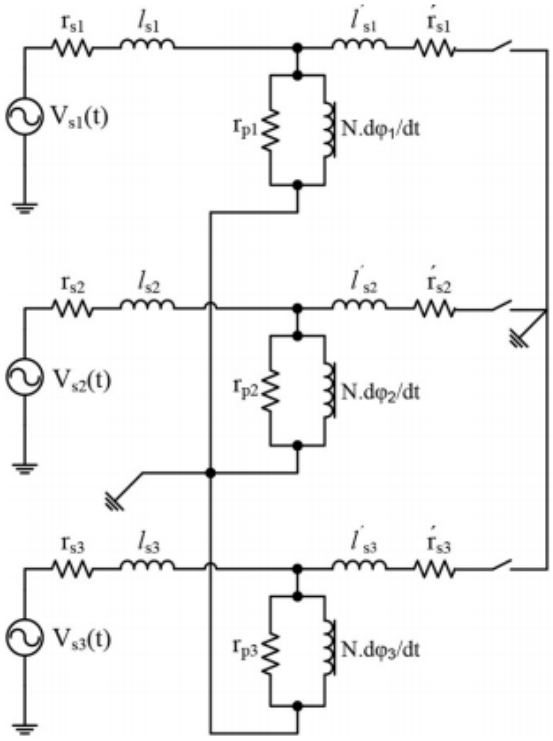

Fig.1. Three phase transformer electrical circuit [27]

Matrices of the winding resistances and inductances are defined as:

$$[R] = \begin{bmatrix} r_{s1} & 0 & 0 \\ 0 & r_{s2} & 0 \\ 0 & 0 & r_{s3} \end{bmatrix} \quad (1)$$

$$[L] = \begin{bmatrix} l_{s1} & m_{12} & m_{13} \\ m_{21} & l_{s2} & m_{23} \\ m_{31} & m_{32} & l_{s3} \end{bmatrix} \quad (2)$$

Where l_{s1},l_{s2} and l_{s3} are leakage inductance (H), and m_{12},m_{23} and m_{31} are mutual inductance (H). The current i_ψ (t) must be expressed in a nonlinear way in Figure 1. Therefore, the magnetizing current is considered as [28]:

$$i_\psi(t) = 0.7576\,\psi(t) + 1.03 \times 10^7 \psi^{19}(t) \quad (3)$$

Equations (4) to (7) describe the three phase circuit of the Figure 1 as:

$$\begin{aligned} v_{s1}(t) &= r_{s1} i_{inr1}(t) + l_{s1}\frac{di_{inr1}(t)}{dt} + m_{12}\frac{di_{inr2}(t)}{dt} \\ &+ m_{13}\frac{di_{inr3}(t)}{dt} + v_1(t) = r_{s1} i_{inr1}(t) + l_{s1}\frac{di_{inr1}(t)}{dt} \\ &+ m_{12}\frac{di_{inr2}(t)}{dt} + m_{13}\frac{di_{inr3}(t)}{dt} + \frac{d\psi_1}{dt} \end{aligned} \quad (4)$$

$$\begin{aligned} v_{s2}(t) &= r_{s2} i_{inr2}(t) + l_{s2}\frac{di_{inr2}(t)}{dt} + m_{21}\frac{di_{inr1}(t)}{dt} \\ &+ m_{23}\frac{di_{inr3}(t)}{dt} + v_2(t) = r_{s2} i_{inr2}(t) + l_{s2}\frac{di_{inr2}(t)}{dt} \\ &+ m_{21}\frac{di_{inr1}(t)}{dt} + m_{23}\frac{di_{inr3}(t)}{dt} + \frac{d\psi_2}{dt} \end{aligned} \quad (5)$$

$$\begin{aligned} v_{s3}(t) &= r_{s3} i_{inr3}(t) + l_{s3}\frac{di_{inr3}(t)}{dt} + m_{31}\frac{di_{inr1}(t)}{dt} \\ &+ m_{32}\frac{di_{inr2}(t)}{dt} + v_3(t) = r_{s3} i_{inr3}(t) + l_{s3}\frac{di_{inr3}(t)}{dt} \\ &+ m_{31}\frac{di_{inr1}(t)}{dt} + m_{32}\frac{di_{inr2}(t)}{dt} + \frac{d\psi_3}{dt} \end{aligned} \quad (6)$$

$$i_{inrj}(t) = \frac{v_j(t)}{r_{mag}} + i_{\psi j}(t) = \frac{1}{r_{mag}}\frac{d\psi_j}{dt} + i_{\psi j}(t),\ \text{j=1,2,3} \quad (7)$$

Therefore, transformer state space model is given as:

$$\begin{bmatrix} l_{s1} & m_{12} & m_{13} & 1 & 0 & 0 \\ m_{21} & l_{s2} & m_{23} & 0 & 1 & 0 \\ m_{31} & m_{32} & l_{s3} & 0 & 0 & 1 \\ 0 & 0 & 0 & \frac{-1}{r_{mag}} & 0 & 0 \\ 0 & 0 & 0 & 0 & \frac{-1}{r_{mag}} & 0 \\ 0 & 0 & 0 & 0 & 0 & \frac{-1}{r_{mag}} \end{bmatrix} \times \underbrace{\begin{bmatrix} \frac{di_{inr1}(t)}{dt} \\ \frac{di_{inr2}(t)}{dt} \\ \frac{di_{inr3}(t)}{dt} \\ \frac{d\psi_1(t)}{dt} \\ \frac{d\psi_2(t)}{dt} \\ \frac{d\psi_3(t)}{dt} \end{bmatrix}}_{\dot{x}} =$$

$$\begin{bmatrix} -r_{s1} & 0 & 0 & 0 & 0 & 0 \\ 0 & -r_{s2} & 0 & 0 & 0 & 0 \\ 0 & 0 & -r_{s3} & 0 & 0 & 0 \\ -1 & 0 & 0 & 0 & 0 & 0 \\ 0 & -1 & 0 & 0 & 0 & 0 \\ 0 & 0 & -1 & 0 & 0 & 0 \end{bmatrix} \times \underbrace{\begin{bmatrix} i_{inr1}(t) \\ i_{inr2}(t) \\ i_{inr3}(t) \\ \psi_1(t) \\ \psi_2(t) \\ \psi_3(t) \end{bmatrix}}_{x}$$

$$+ \begin{bmatrix} 1 & 0 & 0 & 0 & 0 & 0 \\ 0 & 1 & 0 & 0 & 0 & 0 \\ 0 & 0 & 1 & 0 & 0 & 0 \\ 0 & 0 & 0 & 1 & 0 & 0 \\ 0 & 0 & 0 & 0 & 1 & 0 \\ 0 & 0 & 0 & 0 & 0 & 1 \end{bmatrix} \times \underbrace{\begin{bmatrix} v_{s1}(t) \\ v_{s2}(t) \\ v_{s3}(t) \\ i_{\psi 1}(t) \\ i_{\psi 2}(t) \\ i_{\psi 3}(t) \end{bmatrix}}_{u} \quad (8)$$

where v_s(t) is the voltage applied to the transformer primary and ψ(t) is the core flux-turn (Wb.t). we can define:

$$A=\begin{bmatrix} l_{s1} & m_{12} & m_{13} & 1 & 0 & 0 \\ m_{21} & l_{s2} & m_{23} & 0 & 1 & 0 \\ m_{31} & m_{32} & l_{s3} & 0 & 0 & 1 \\ 0 & 0 & 0 & \frac{-1}{r_{mag}} & 0 & 0 \\ 0 & 0 & 0 & 0 & \frac{-1}{r_{mag}} & 0 \\ 0 & 0 & 0 & 0 & 0 & \frac{-1}{r_{mag}} \end{bmatrix}^{-1} \times \begin{bmatrix} -r_{s1} & 0 & 0 & 0 & 0 & 0 \\ 0 & -r_{s2} & 0 & 0 & 0 & 0 \\ 0 & 0 & -r_{s3} & 0 & 0 & 0 \\ -1 & 0 & 0 & 0 & 0 & 0 \\ 0 & -1 & 0 & 0 & 0 & 0 \\ 0 & 0 & -1 & 0 & 0 & 0 \end{bmatrix} \tag{9}$$

$$= \begin{bmatrix} L & I_{3\times3} \\ 0 & \frac{-1}{r_{mag}} I_{3\times3} \end{bmatrix}^{-1} \times \begin{bmatrix} -R & 0 \\ -I & 0 \end{bmatrix}$$

$$= \begin{bmatrix} L^{-1} & r_{mag}L^{-1} \\ 0 & -r_{mag}I \end{bmatrix} \times \begin{bmatrix} -R & 0 \\ -I & 0 \end{bmatrix}$$

$$= \begin{bmatrix} -(L^{-1}R + r_{mag}L^{-1}) & 0 \\ r_{mag}I & 0 \end{bmatrix}$$

$$B=\begin{bmatrix} l_{s1} & m_{12} & m_{13} & 1 & 0 & 0 \\ m_{21} & l_{s2} & m_{23} & 0 & 1 & 0 \\ m_{31} & m_{32} & l_{s3} & 0 & 0 & 1 \\ 0 & 0 & 0 & \frac{-1}{r_{mag}} & 0 & 0 \\ 0 & 0 & 0 & 0 & \frac{-1}{r_{mag}} & 0 \\ 0 & 0 & 0 & 0 & 0 & \frac{-1}{r_{mag}} \end{bmatrix}^{-1} \tag{10}$$

$$\times \underbrace{\begin{bmatrix} 1 & 0 & 0 & 0 & 0 & 0 \\ 0 & 1 & 0 & 0 & 0 & 0 \\ 0 & 0 & 1 & 0 & 0 & 0 \\ 0 & 0 & 0 & 1 & 0 & 0 \\ 0 & 0 & 0 & 0 & 1 & 0 \\ 0 & 0 & 0 & 0 & 0 & 1 \end{bmatrix}}_{I_{6\times6}} = \begin{bmatrix} L^{-1} & r_{mag}L^{-1} \\ 0 & -r_{mag}I \end{bmatrix}$$

$$C = I_{6\times6} \tag{11}$$

Therefore, we have:

$$\begin{aligned} \dot{x} &= Ax + Bu \\ y &= Cx \end{aligned} \tag{12}$$

The state space model in equation (1) is continuous in time. But, to implement the extended Kalman filter, we need a discrete time model. By discretizing the derivatives, we have:

$$\frac{di_{inrj}(t)}{dt} \approx \frac{i_{inrj}(t+\Delta t)-i_{inrj}(t)}{\Delta t} \tag{13}$$

$$\frac{d\psi_{inrj}(t)}{dt} = \frac{\psi_{inrj}(t+\Delta t)-\psi_{inrj}(t)}{\Delta t} \tag{14}$$

Now, we substitute these discrete derivatives into the original equations and rearranging the equations. Equation (3) shows the discrete state space model as follows:

$$\begin{bmatrix} r_{s1}\Delta t + l_{s1} & m_{12} & m_{13} & 1 & 0 & 0 \\ m_{21} & r_{s2}\Delta t + l_{s2} & m_{23} & 0 & 1 & 0 \\ m_{31} & m_{32} & r_{s3}\Delta t + l_{s3} & 0 & 0 & 1 \\ r_{mag}\Delta t & 0 & 0 & -1 & 0 & 0 \\ 0 & r_{mag}\Delta t & 0 & 0 & -1 & 0 \\ 0 & 0 & r_{mag}\Delta t & 0 & 0 & -1 \end{bmatrix} \times \begin{bmatrix} i_{inr1}(t+\Delta t) \\ i_{inr2}(t+\Delta t) \\ i_{inr3}(t+\Delta t) \\ \psi_1(t+\Delta t) \\ \psi_2(t+\Delta t) \\ \psi_3(t+\Delta t) \end{bmatrix} = \tag{15}$$

$$\begin{bmatrix} v_{s1}(t)\Delta t + l_{s1}i_{inr1}(t) + m_{12}i_{inr2}(t) + m_{13}i_{inr3}(t) + \psi_1(t) \\ v_{s2}(t)\Delta t + m_{21}i_{inr1}(t) + l_{s2}i_{inr2}(t) + m_{23}i_{inr3}(t) + \psi_2(t) \\ v_{s3}(t)\Delta t + m_{31}i_{inr1}(t) + m_{32}i_{inr2}(t) + l_{s3}i_{inr3}(t) + \psi_3(t) \\ i_{\psi1}(t)\left(r_{mag}\Delta t\right) - \psi_1(t) \\ i_{\psi2}(t)\left(r_{mag}\Delta t\right) - \psi_2(t) \\ i_{\psi3}(t)\left(r_{mag}\Delta t\right) - \psi_3(t) \end{bmatrix}$$

The equivalent circuit of the transformer for the delta-connected windings is shown in Figure 2. Where Ψ_k is flux linkage associated with the transformer's primary coil, in the k-th column of the transformer, $i_k^{(g)}$ is transformer primary current, $R_{Fe,k}$ is equivalent resistance representing the iron core losses, $i_{Fe,k}$ is active component of the transformer's idle current, R_s is equivalent resistance of the power grid (power source), L_s is equivalent inductance (reactance) of the power grid (power source), Rg is primary winding resistance, L_g is leakage inductance of the primary winding, Φ is main flux leakage (effective value of the flux), N_g is number of turns in the primary windings. Equations for three independent circulations appeared as a result of applying Kirchhoff's second law to the modeled equivalent circuits of the primary side of the transformer are:

$$\begin{aligned} &-R_s i_1^s(t) - L_s\frac{di_1^s(t)}{dt} + R_s i_2^s(t) + L_s\frac{di_2^s(t)}{dt} \\ &+R_g i_2^{(g)}(t) + L_g\frac{di_2^{(g)}(t)}{dt} + \frac{d\psi_2(t)}{dt} = e_{12}^{(s)}(t) \end{aligned} \tag{16}$$

$$\begin{aligned} &-R_s i_2^s(t) - L_s\frac{di_2^s(t)}{dt} + R_s i_3^s(t) + L_s\frac{di_3^s(t)}{dt} \\ &+R_g i_3^{(g)}(t) + L_g\frac{di_3^{(g)}(t)}{dt} + \frac{d\psi_3(t)}{dt} = e_{23}^{(s)}(t) \end{aligned} \tag{17}$$

$$\begin{aligned} &R_g i_1^{(g)}(t) + L_g\frac{di_1^{(g)}(t)}{dt} + R_g i_2^{(g)}(t) + L_g\frac{di_2^{(g)}(t)}{dt} \\ &+R_g i_3^{(g)}(t) + L_g\frac{di_3^{(g)}(t)}{dt} \\ &+\frac{d\psi_1(t)}{dt} + \frac{d\psi_2(t)}{dt} + \frac{d\psi_3(t)}{dt} = 0 \end{aligned} \tag{18}$$

where

$$\begin{aligned} i_1^s(t) &= i_1^{(g)}(t) - i_2^{(g)}(t) \\ i_2^s(t) &= i_2^{(g)}(t) - i_3^{(g)}(t) \\ i_3^s(t) &= i_3^{(g)}(t) - i_1^{(g)}(t) \end{aligned} \tag{19}$$

The resulting system of equations is ordered in matrix form:

$$\begin{bmatrix} -L_s & 2L_s+L_g & -L_s \\ -L_s & -L_s & 2L_s+L_g \\ L_g & L_g & L_g \end{bmatrix} \times \begin{bmatrix} \frac{di_1^{(g)}(t)}{dt} \\ \frac{di_2^{(g)}(t)}{dt} \\ \frac{di_3^{(g)}(t)}{dt} \end{bmatrix} = \begin{bmatrix} R_s & -2R_s-R_g & -R_s \\ R_s & R_s & -2R_s-R_g \\ -R_g & -R_g & -R_g \end{bmatrix} \begin{bmatrix} i_1^{(g)}(t) \\ i_2^{(g)}(t) \\ i_3^{(g)}(t) \end{bmatrix} - \begin{bmatrix} \frac{d\psi_2(t)}{dt} \\ \frac{d\psi_3(t)}{dt} \\ 0 \end{bmatrix} + \begin{bmatrix} e_{12}^{(s)}(t) \\ e_{23}^{(s)}(t) \\ 0 \end{bmatrix} \quad (20)$$

Using the circuit description in modeling the magnetic circuit of the transformer, we can state that:

$$\frac{d\psi_k(t)}{dt} = R_{Fe,k} i_{Fe,k}(t) \quad (21)$$

Taking into account Kirchhoff's first and second laws for the magnetic circuit of the transformer, we have:

$$\left(\frac{1}{R_{Fe1}} + \frac{1}{R_{Fe2}}\right)\frac{d\psi_2(t)}{dt} + \frac{1}{R_{Fe1}}\frac{d\psi_3(t)}{dt} = i_2^{(g)}(t) - i_1^{(g)}(t) - \frac{U_{m,1}}{N_g}(\psi_2(t)+\psi_3(t)) - \frac{U_{m,2}}{N_g}\psi_2(t) \quad (22)$$

$$\frac{1}{R_{Fe2}}\frac{d\psi_2(t)}{dt} - \frac{1}{R_{Fe3}}\frac{d\psi_3(t)}{dt} = i_3^{(g)}(t) - i_2^{(g)}(t) - \frac{U_{m,2}}{N_g}\psi_2(t) + \frac{U_{m,3}}{N_g}\psi_3(t) \quad (23)$$

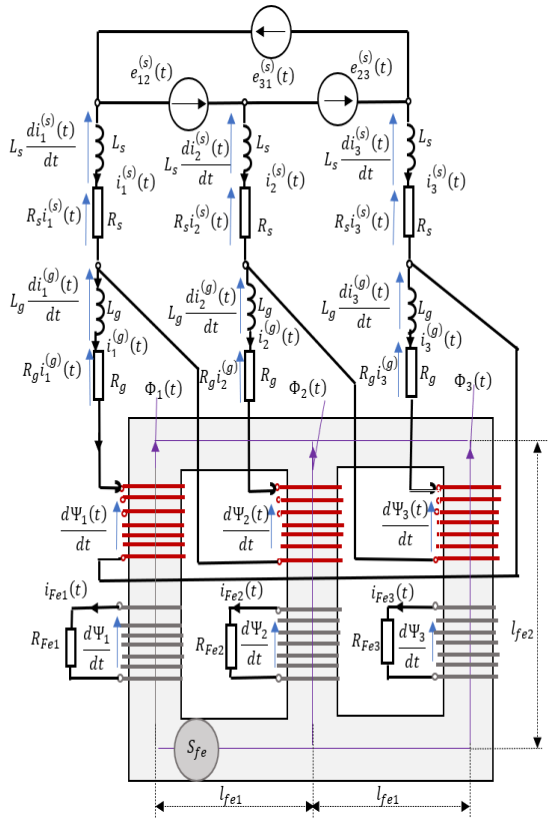

Fig.2. Equivalent circuit of the D-y three-phase transformer

III. Extended Kalman Filter and Inrush Current Simulation Results

The Kalman filter was introduced in 1961 by Rudolph Kalman (Hungarian-American electrical engineer and mathematician) and Bossi. This filter is a mathematical technique that is widely used in digital signal processing, navigation and control systems [29]. In fault location or satellite position detection, detection based methods use fewer sensors and have lower cost and more reliability than the other methods. In some situations, the estimation of the state variables can be more efficient than the direct measurement of them due to the effect of the noise phenomenon in the measurement. Kalman filter is a powerful tool for extracting information in the presence of uncertainties and provides an optimal solution for tracking and forecasting problems.

Kalman filter (KF) is applied for linear systems and provides optimal estimates for linear systems, while the extended Kalman filter (EKF) is an extension that can be applied to nonlinear systems and provides approximate estimates for nonlinear systems. The EKF works by transforming the nonlinear models at each time step into linearized systems of Equations. In a single-variable model, you would do this using the current model value and its derivative; the generalization for multiple variables and Equations is the Jacobian matrix. The linearized Equations are then used in a similar manner to the standard Kalman filter. If you have a bad initial guess of the underlying system's state, in many cases where you approximate a nonlinear system with a linear model, the EKF will not perform well. The EKF is merely an extension of the linear-system technique to a wider class of problems. The nonlinear EKF model of the system can be represented as follows:

$$\begin{aligned} \dot{x} &= f(x, V(t), \omega, t) \\ \bar{y} &= \bar{h}(\bar{x}, \bar{v}, \bar{t}) \\ \bar{\omega} &= (\bar{0}, \bar{Q}) \\ \bar{v} &= (\bar{0}, \bar{R}) \end{aligned} \quad (24)$$

In Equation (24), v and ω are uncorrelated white noises with zero mean and x is the state vector. Moreover, $\omega 0$ and $v0$ are zero. y and v are the transformer measured inrush current and input voltage. Moreover, Q and R matrices are chosen as follows:

$$Q = \begin{bmatrix} 0.2 & 0 & 0 & 0 & 0 & 0 \\ 0 & 0.05 & 0 & 0 & 0 & 0 \\ 0 & 0 & 0.5 & 0 & 0 & 0 \\ 0 & 0 & 0 & 0.2 & 0 & 0 \\ 0 & 0 & 0 & 0 & 0.05 & 0 \\ 0 & 0 & 0 & 0 & 0 & 0.5 \end{bmatrix} \quad (25)$$

$$R = I_{6\times 6} \quad (26)$$

Therefore,

$$f(x,V(t),\omega,t) = Ax + Bu + \omega$$
$$= \begin{bmatrix} -(L^{-1}R + r_{mag}L^{-1}) & 0 \\ r_{mag}I & 0 \end{bmatrix} x + \begin{bmatrix} L^{-1} & r_{mag}L^{-1} \\ 0 & -r_{mag}I \end{bmatrix} u + \omega \quad (27)$$

$$h(x,v,t) = Cx + v \quad (28)$$

$$F = \frac{\partial f}{\partial x}$$

$$= \begin{bmatrix} -(L^{-1}R + r_{mag}L^{-1}) & r_{mag}L^{-1} \times \begin{bmatrix} \frac{\partial i_{\psi 1}}{\partial \psi_1} & \frac{\partial i_{\psi 2}}{\partial \psi_2} & \frac{\partial i_{\psi 3}}{\partial \psi_3} \\ \frac{\partial i_{\psi 1}}{\partial \psi_1} & \frac{\partial i_{\psi 2}}{\partial \psi_2} & \frac{\partial i_{\psi 3}}{\partial \psi_3} \\ \frac{\partial i_{\psi 1}}{\partial \psi_1} & \frac{\partial i_{\psi 2}}{\partial \psi_2} & \frac{\partial i_{\psi 3}}{\partial \psi_3} \end{bmatrix} \\ r_{mag}I & -r_{mag} \begin{bmatrix} \frac{\partial i_{\psi 1}}{\partial \psi_1} & \frac{\partial i_{\psi 2}}{\partial \psi_2} & \frac{\partial i_{\psi 3}}{\partial \psi_3} \\ \frac{\partial i_{\psi 1}}{\partial \psi_1} & \frac{\partial i_{\psi 2}}{\partial \psi_2} & \frac{\partial i_{\psi 3}}{\partial \psi_3} \\ \frac{\partial i_{\psi 1}}{\partial \psi_1} & \frac{\partial i_{\psi 2}}{\partial \psi_2} & \frac{\partial i_{\psi 3}}{\partial \psi_3} \end{bmatrix} \end{bmatrix} \quad (29)$$

$$L = \frac{\partial f}{\partial \omega} = I_{6\times 6} \quad (30)$$

$$H = \frac{\partial h}{\partial x} = C \quad (31)$$

$$M = \frac{\partial \bar{h}}{\partial v} = I_{6\times 6} \quad (32)$$

To realize the EKF filter, the state variable and the estimation error covariance matrix are initialized as:

$$\hat{x}_0 = E(x_0) \quad (33)$$

$$P = P_0 = E\{(x_0 - \hat{x}_0)(x_0 - \hat{x}_0)^T\} \quad (34)$$

where E is mathematical expectation of variable and P is the estimation error covariance matrix. The estimation equations are stated as:

$$K = P \times H^T \times (M \times R \times M^T)^{-1} \quad (35)$$

$$\hat{\dot{x}} = f(\hat{x},V(t),\omega_0,t) + K \times (y - h(\hat{x},v_0,t)) \quad (36)$$

Where K is the estimator gain. Updating equation is:

$$\dot{P} = F \times P + P \times F^T + L \times Q \times L^T - K \times C \times P \quad (37)$$

To calculate the inrush current, equation (15) must be solved using MATLAB software. It should be noted that the three phase currents of the primary side and the value of the windings flux are as 6 state variables in equation (15). The specifications of the studied transformer have been brought in Table 1.

Table 1. Specifications of the first studied transformer

Name	Value
Voltage of phase a	$V_a(t) = 110\cos(\omega t - \alpha)$
Voltage of phase b	$V_a(t) = 110\cos(\omega t - (120° + \alpha))$
Voltage of phase c	$V_b(t) = 110\cos(\omega t - (240° + \alpha))$
Switching angle	$\alpha = 42.97°$
Power	4.5 kVA
Frequency	50 Hz

After the inrush current calculations, we have to implement the EKF filter. The filter can be useful if its estimation of the current, with an error close to zero, is consistent with the current of the previous step. This filter is implemented on the transformer state equations. The inrush currents are shown in figure 3.

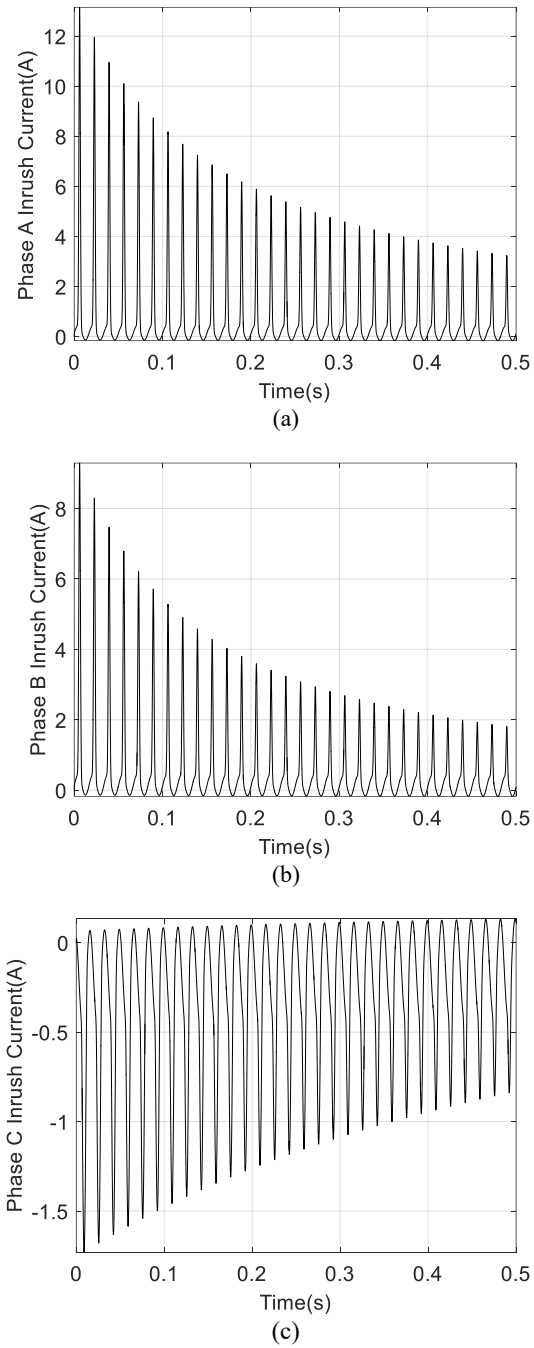

Fig. 3. Inrush currents of the transformer; a) Phase A, b) Phase B, c) Phase C

IV. Fault Current Simulation

External and internal faults are two general classes of electrical faults in the transformer. External faults are not related to the transformer itself, but they directly affect it. Internal faults also occur inside the transformer and are related to the equipment of the transformer. Among the internal faults, we can mention phase-to-phase connection of the windings, connection of the phase to the ground, turn to

turn fault in the winding [30]. In this section, connection of the winding to the ground is considered. In the following, in the presence of this fault, transformer inrush current is simulated, and then the results of the inrush current estimation are proposed. Finally, by comparing the calculated/measured current and the estimated current, the estimation error signal or the residual signal is obtained, and at that time, a decision is made about the fault condition or the normal condition of the transformer. Then, if the fault current is detected, using the β index, location of the fault in the winding is determined. If a ground connection fault occurs in one of the windings, it divides the winding into two parts and causes the resistance and inductance matrices to be 7×7 matrices:

$$[R]=\begin{bmatrix} R_1 & 0 & 0 & 0 & 0 & 0 & 0 \\ 0 & R_2 & 0 & 0 & 0 & 0 & 0 \\ 0 & 0 & R_a & 0 & 0 & 0 & 0 \\ 0 & 0 & 0 & R_b & 0 & 0 & 0 \\ 0 & 0 & 0 & 0 & R_4 & 0 & 0 \\ 0 & 0 & 0 & 0 & 0 & R_5 & 0 \\ 0 & 0 & 0 & 0 & 0 & 0 & R_6 \end{bmatrix} \quad (38)$$

$$[L]=\begin{bmatrix} L_1 & M_{12} & M_{1a} & M_{1b} & M_{14} & M_{15} & M_{16} \\ M_{21} & L_2 & M_{2a} & M_{2b} & M_{24} & M_{25} & M_{26} \\ M_{a1} & M_{a2} & L_a & M_{ab} & M_{a4} & M_{a5} & M_{a6} \\ M_{b1} & M_{b2} & M_{ba} & L_b & M_{b4} & M_{b5} & M_{b6} \\ M_{41} & M_{42} & M_{4a} & M_{4b} & L_4 & M_{45} & M_{46} \\ M_{51} & M_{52} & M_{5a} & M_{5b} & M_{54} & L_5 & M_{56} \\ M_{61} & M_{62} & M_{6a} & M_{6b} & M_{64} & M_{65} & L_6 \end{bmatrix} \quad (39)$$

The fault in the winding has caused to have the number of N_a turns of the winding in the upper part and N_b turns of the winding in the lower part of the winding. The unknown resistances R_a and R_b are given as**:**

$$R_a=\frac{N_a}{N_3}R_3\,,R_b=\frac{N_b}{N_3}R_3 \quad (40)$$

The other unknown values in the equation (39) are brought as follows:

$$a=\frac{N_a}{N_b} \quad (41)$$

$$L_a=\frac{a^2L_3}{a^2+2a+1} \quad (42)$$

$$L_b=\frac{L_3}{a^2+2a+1} \quad (43)$$

$$M_{ab}=\frac{aL_3}{a^2+2a+1} \quad (44)$$

$$M_{3i}=M_{ai}+M_{bi} \quad (45)$$

$$\frac{M_{ai}}{M_{bi}}=a \quad (46)$$

$$M_{ai}=\frac{a}{1+a}\times M_{3i} \quad (47)$$

$$M_{bi}=\frac{1}{1+a}\times M_{3i} \quad (48)$$

Therefore, the resistance and inductance matrices of the transformer in the section 2 considering connection of winding to the ground are given as:

$$[R]=\begin{bmatrix} R_1 & 0 & 0 & 0 \\ 0 & R_a & 0 & 0 \\ 0 & 0 & R_b & 0 \\ 0 & 0 & 0 & R_3 \end{bmatrix} \quad (49)$$

$$[L]=\begin{bmatrix} L_1 & M_{1a} & M_{1b} & M_{13} \\ M_{a1} & L_a & M_{ab} & M_{a3} \\ M_{b1} & M_{ba} & L_b & M_{b3} \\ M_{31} & M_{3a} & M_{3b} & L_3 \end{bmatrix} \quad (50)$$

Because the resistance and inductance values change depending on the location of the fault, unknown values in (49) and (50) are calculated for 9 positions of the winding connection to the ground. These values have been considered in the upper 10% of the winding to the lower 10% of the winding respectively. It should be noted that the fault is considered in the middle phase and the transformer windings connection is star-shaped. According to the new resistance and inductance values in the fault conditions, it is possible to calculate the fault current during the startup of the transformer in every 10% of the winding. The inrush current estimation in the fault mode is also done using the EKF formulation. It should be noted that the simulation has been performed at switching angle 42.97°. Figure 4 shows the difference between measured and estimated current in faulty transformer which the fault occurs in the upper 10% of the winding. The difference between the actual and estimated inrush current for the faulty transformer with the location of the fault in the half of the winding have been shown in figure 5. As it can be seen from the simulation results, depending on the location of the fault, there is always a percentage of estimation error between the measured and the estimated signal. Figure 6 shows the difference between measured and estimated current in faulty transformer which the fault occurs in the lower 10% of the winding. As it can be seen in figure 6, in this the location of the fault, the fault current is very close to the normal inrush current.

V. Discriminating the Fault from the Inrush Current and the Winding Fault Location

a) The estimation error standard deviation

In this section, the covariance matrix of the estimation error is introduced in order to determine when the error becomes close to zero. In order to check the estimation error changes relative to time, the trace of estimation error covariance matrix is used. The trace of a matrix, which is defined only for square matrices, is equal to the sum of the eigenvalues of the matrix.

$$trace(A)=\sum\lambda_i \quad (51)$$

It can be shown that the estimation error starts from 0.01 at the beginning and increases, but after a period of time (about 10 milliseconds), it reaches its final value. Estimation error covariance matrix is used to monitor the steady state estimation error value. On the other hand, to obtain the estimation error in the steady state, the standard deviation index is also used so that in addition to the covariance matrix, which provides an intuitive view of the estimation error, a comparable numerical index is also available.

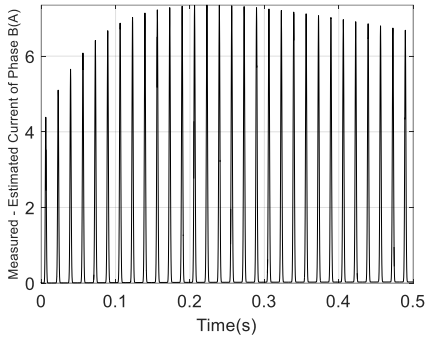

Fig. 4. Difference between measured and estimated current with the location of the fault in the upper 10% of the winding in phase B of the transformer

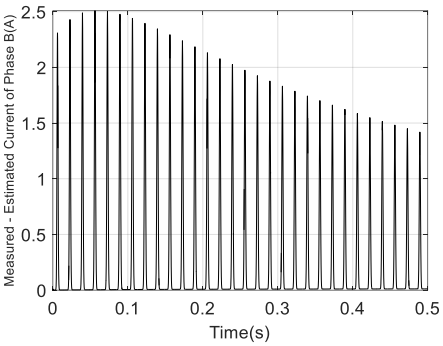

Fig. 5. Difference between measured and estimated current with the location of the fault in the half of the winding in phase B of the transformer

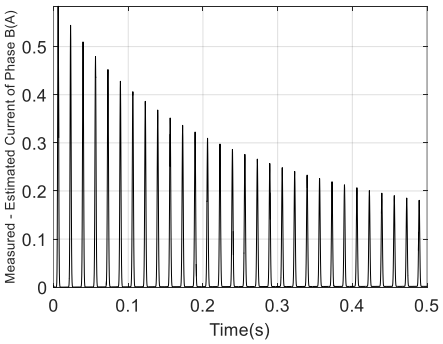

Fig. 6. Difference between measured and estimated current with the location of the fault in the lower 10% of the winding in phase B of the transformer

The standard deviation is the root of the variance. Variance is defined as the average value of the square of the differences of the values from the mean. Standard deviation is one of the dispersal indicators so that shows the data how far from the average value. The estimation error standard deviation of the transformer fault current in phases a, b and c are equal to 0.004, 0.01 and 0.02 respectively. In the previous section, the simulation results showed that the estimated current of the transformer is almost the same as the measured current in the healthy transformer, and the estimation error eventually tended to zero. On the other hand, it was shown that in a faulty transformer, there is always a significant difference between the estimated and the measured inrush current relative to the location of the fault. But in order to obtain the numerical value of this difference and to discriminate between the normal inrush current and the fault current, a numerical index is required. Table 2 shows the estimation error standard deviation of the healthy three phase transformer at different switching angles.

Table 2. The estimation error standard deviation of the healthy transformer

Switching angle(°)	Phase A	Phase B	Phase C
5	0.004	0.01	0.02
42.97	0.01	0.008	0.01
80	0.05	0.07	0.06

Figure 7 shows the estimation error standard deviation of the faulty three phase transformer at different switching angles with 9 separate locations of the fault in the winding of the phase B. The standard deviation index at different switching angles does not show a constant value to identify the location of the fault. To solve this problem, an index β is defined so that it is equal to the second norm of the inrush current vector divided by the standard deviation of the estimation error. The estimation error is equal to the difference between the measured and the estimated inrush current:

$$\hat{\imath}_{inr} = i_{inr,meas} - i_{inr,est} \tag{52}$$

Therefore, the standard deviation of the estimation error is calculated as:

$$i_{inr,sd} = \sqrt{\frac{\sum_{j=1}^{N} (\hat{\imath}_{inr}(j) - \hat{\imath}_{inr,mean})^2}{N}} \tag{53}$$

Where:

$$\hat{\imath}_{inr,mean} = \frac{\hat{\imath}_{inr1} + \hat{\imath}_{inr2} + \cdots \hat{\imath}_{inrN}}{N} \tag{54}$$

Index β is given as:

$$\beta = \frac{\sqrt{\sum_{j=1}^{N} i_{inr}^2(j)}}{i_{inr,sd}} \times 100 = \frac{\sqrt{\sum_{j=1}^{N} i_{inr}^2(j)}}{\sqrt{\frac{\sum_{j=1}^{N} (\hat{\imath}_{inr}(j) - \hat{\imath}_{inr,mean})^2}{N}}} \times 100 \tag{55}$$

This index has been calculated in Table 3 in the healthy transformer at three different switching angles. On the other hand, this index has been calculated in Table 4 in the faulty transformer, with 9 separate locations of the fault in the winding, and with three different switching angles.

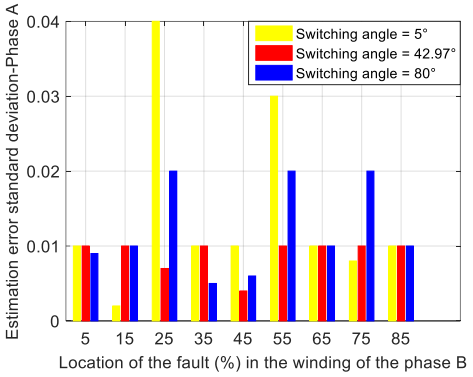

(a)

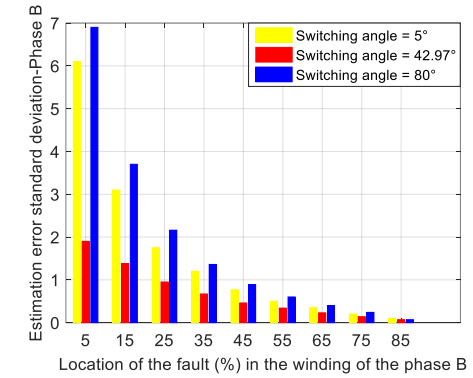

(b)

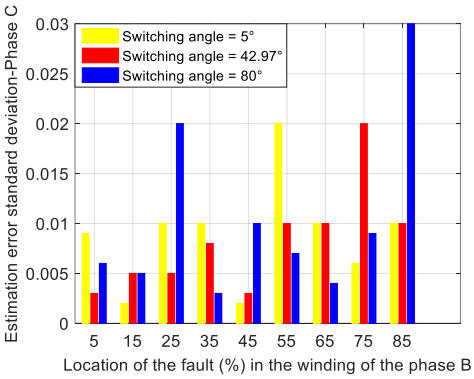

(c)

Fig. 7. The estimation error standard deviation of the faulty transformer at different switching angles; a) Phase A, b) Phase B, c) Phase C

The estimation error in table 2 shows that in the healthy transformer (phase B), the maximum value of the estimation error is 0.01, on the other hand in the faulty transformer with different percentages of error, the minimum value is 0.07. Therefore, it is possible to use the estimation error standard deviation index to determine whether the transformer is faulty or is not. Its adjustment value is set at 0.05 in this paper. In this way, if the value of this index is greater than 0.05 in any phase, it can be shown that there is a fault condition. The index β in table 3 shows that for a healthy transformer (phase B), the minimum value of this index is 6.2%. The maximum value of this index is 5.9% for the faulty phase with the location of the fault in 90% of the winding. Therefore, it is possible to classify the location of the fault in the table 5.

Table.3.The index β of the healthy transformer

Switching angle(°)	Phase A	Phase B	Phase C
5	٣٤,٢	٨٥,١	٥,٥
42.97	٢٧,٦	٦,٢	٢٩,٤
80	٢٤,٣	٧٨	٧,٤

Table.4.The index β of the faulty transformer

Location of the fault (%) in the winding of phase B	Switching angle(°)	Phase A	Phase B	Phase C
	5	١٣,٨	٠,٤	١٢
Upper 10%	42.97	٢٧,٩	٠,٤٩	٣٩,٣
	80	٧,٤	٠,٤١	١٣
	5	٦٨,٥	٠,٥١	٥٣,٥
10 to 20	42.97	٢٨,٥	٠,٥٣	١٢
	80	٦,٧	٠,٥١	١٤,٨
	5	٦,٧٥	٠,٥٥	١٠,٧
20 to 30	42.97	٤٠,٢	٠,٥٩	٢٣,٢
	80	٣,٣٥	٠,٥٣	٣,٧
	5	١٣,٨	٠,٦٣	١٠,٦
30 to 40	42.97	٢٨,٥	٠,٦٩	١٤,٧٥
	80	١٣,٤	٠,٦٤	٢٤,٦
	5	١٣,٦	٠,٧٩	٥,٥
40 to 50	42.97	٧٠	٠,٨٦	٣٩,٤
	80	١١,١	٠,٧٩	٧,٤
	5	٤,٥	١	٥,٣٥
50 to 60	42.97	٢٨,٧	١,١	١١٨
	80	٣,٣٥	١	١٠,٥
	5	١٣,٨	١,٣	١٠,٦
60 to 70	42.97	٢٨,٨	١,٤٦	١١,٧
	80	٦,٧	١,٣٢	١٨,٥
	5	١٧,٣	٢	١٧,٦
70 to 80	42.97	٢٧,٨	٢,١٦	٥٩
	80	٣,٣٥	١,٩٧	٨,٢
	5	١٣,٦	٣,٢	١٠,٦
80 to 90	42.97	٢٨,٤	٤	١٢
	80	٦,٧	٥,٩	٢,٤٦

Table 5. The location of the fault classification in faulty phase of the transformer

The location of the fault in the winding (%)	Index β (%)
Upper 10%	0.4 <β< 0.49
10 to 20	0.5 <β< 0.54
20 to 30	0.55 <β< 0.59
30 to 40	0.6 <β< 0.69
40 to 50	0.7 <β< 0.89
50 to 60	0.9 <β< 1.1
60 to70	1.2 <β< 1.6
70 to 80	1.7 <β< 2.8
80 to 90	2.9<β< 6.0

b) Validation of the results

Table 6 shows comparison of the other references in fault detection and location as follows:

Table 6. Comparison of the other references in fault detection and location

Ref.	Method	Transformer	Fault type	Location capability	Measurement
[7]	FRA	A winding	Turn-to-turn	Yes	Yes
[11]	Wavelet Transform	Three phase	Winding to the	Yes	No
[15]	Neural Network	Single phase	Winding to the	No	No
[16]	EKF	Single Phase	Winding to the	No	No
[17]	EKF	Single Phase	Winding to the	No	Yes
[20]	Hermite transform	Three phase	Internal faults	No	No
[24]	FRA	Three phase	Internal faults	No	Yes
[25]	FRA	Three phase	Insulation faults	Yes	Yes

The presented method has been validated using the single phase transformer in [17]. The specifications of this transformer have been brought in Table 7.

Table.7. Parameters of the single phase transformer in [17]

Name	Value
Power	15 kVA
Ratio	2300/230
Frequency	50 Hz
Primary winding	3.225 Ω
Primary winding	4.85 Ω
Core resistance	105 k Ω

Equivalent circuit of the transformer is shown in Figure 8.

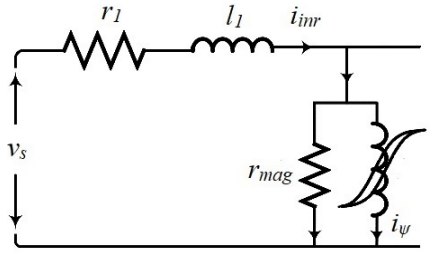

Fig.8. Equivalent circuit of the single phase transformer

It is worth noting that fault localization has not been performed in reference [17]. To identify nonlinear model, Equation (56) has been used for modelling the magnetic core behavior in [17]:

$$i_\psi(t) = 16\psi^5 - 47\psi^4 + 43\psi^3 - 11.5\psi^2 - 0.5\psi + 0.02 \tag{56}$$

State space equations for this single phase transformer is given as follows:

$$\begin{bmatrix} l & 1 \\ 0 & -\frac{1}{r_{mag}} \end{bmatrix} \times \begin{bmatrix} \frac{di_{inr}(t)}{dt} \\ \frac{d\psi(t)}{dt} \end{bmatrix} = \begin{bmatrix} -r & 0 \\ -1 & 0 \end{bmatrix} \times \begin{bmatrix} i_{inr}(t) \\ \psi(t) \end{bmatrix} + \begin{bmatrix} 1 & 0 \\ 0 & 1 \end{bmatrix} \times \begin{bmatrix} v_s(t) \\ i_\psi(t) \end{bmatrix} \tag{57}$$

Or:

$$\underbrace{\begin{bmatrix} \frac{di_{inr}(t)}{dt} \\ \frac{d\psi(t)}{dt} \end{bmatrix}}_{\dot{x}} = \underbrace{\begin{bmatrix} -\frac{r+r_{mag}}{l} & 0 \\ r_{mag} & 0 \end{bmatrix}}_{A} \times \underbrace{\begin{bmatrix} i_{inr}(t) \\ \psi(t) \end{bmatrix}}_{x} + \underbrace{\begin{bmatrix} \frac{1}{l} & \frac{r_{mag}}{l} \\ 0 & -r_{mag} \end{bmatrix}}_{B} \times \underbrace{\begin{bmatrix} v_s(t) \\ i_\psi(t) \end{bmatrix}}_{u} \tag{58}$$

$$y = \underbrace{\begin{bmatrix} 1 & 0 \\ 0 & 1 \end{bmatrix}}_{C} \begin{bmatrix} i_{inr}(t) \\ \psi(t) \end{bmatrix}$$

The nonlinear EKF model of the system can be represented as follows:

$$\begin{aligned} \dot{x} &= f(x, V_s(t), \omega, t) \\ y &= h(x, v, t) \\ \omega &= (0, Q) \\ v &= (0, R) \end{aligned} \tag{59}$$

Matrices Q and R are given as follows [17]:

$$Q = \begin{bmatrix} 0.2 & 0 \\ 0 & 0.5 \end{bmatrix} \tag{60}$$

$$R = 1 \tag{61}$$

We have:

$$f(x, V_s(t), \omega, t) = \begin{bmatrix} -\frac{r+r_{mag}}{l} & 0 \\ r_{mag} & 0 \end{bmatrix} \begin{bmatrix} i_{inr}(t) \\ \psi(t) \end{bmatrix} + \begin{bmatrix} \frac{1}{l} & \frac{r_{mag}}{l} \\ 0 & -r_{mag} \end{bmatrix} \times \begin{bmatrix} v_s(t) \\ i_\psi(t) \end{bmatrix} + \begin{bmatrix} \omega_1 \\ \omega_2 \end{bmatrix} \tag{62}$$

$$h(x, v, t) = \begin{bmatrix} 1 & 0 \\ 0 & 1 \end{bmatrix} \begin{bmatrix} i_{inr}(t) \\ \psi(t) \end{bmatrix} + \begin{bmatrix} v_1 \\ v_2 \end{bmatrix} \tag{63}$$

$$F = \frac{\partial f}{\partial x} = \begin{bmatrix} -\frac{r+r_{mag}}{l} & \frac{r_{mag}}{l} \cdot \frac{\partial i_\psi}{\partial \psi} \\ r_{mag} & -r_{mag} \cdot \frac{\partial i_\psi}{\partial \psi} \end{bmatrix} \tag{64}$$

$$L = \frac{\partial f}{\partial \omega} = \begin{bmatrix} 1 & 0 \\ 0 & 1 \end{bmatrix} \tag{65}$$

$$H = \frac{\partial h}{\partial x} = C \tag{66}$$

$$M = \frac{\partial h}{\partial v} = I_{2\times 2} \tag{67}$$

The residual flux is initially assumed to be zero. Figure 9 shows the inrush current of the transformer with zero residual flux at switching angles 0° (zero voltage). Now the residual flux is assumed to be 20%. Figure 10 shows the inrush current of the transformer with 20% residual flux at switching angles 0°. On the other hand, the proposed method has 9ms mean detection time in distinguishing inrush current from fault current and fault location. Figure 11 shows the inrush current of the transformer with zero residual flux and CT saturation at switching angles 0°. Besides, Figure 12 shows the inrush current of the transformer with 20% residual flux and CT saturation at switching angles 0°.

Table 8 shows the estimation error standard deviation of the second studied transformer in the faulty condition with 9

separate locations of the fault in the winding. To examine the sensitivity and robustness of the proposed method for fault location, we first make 5% change in the transformer resistance and leakage inductance values. Secondly, we apply a 10% change to the noise matrices values in the EKF method. Table 8 shows the percentage of changes in the standard deviation of the estimation error from its previous values. As it can be seen from Table 8, the estimation error standard deviation has a very small deviation from the mentioned changes.

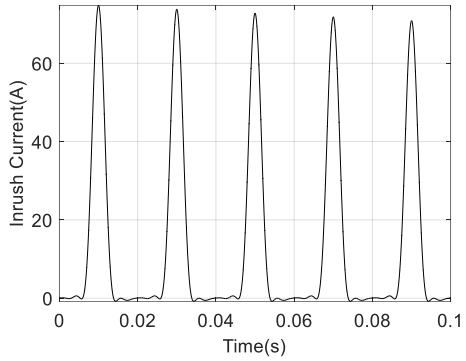

Fig. 9. Transformer Inrush current with zero residual flux at switching angle 0°

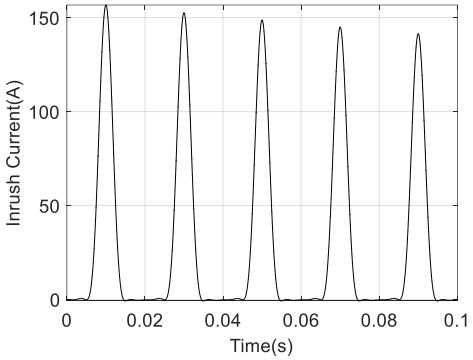

Fig. 10. Transformer Inrush current with 20% residual flux at switching angle 0°

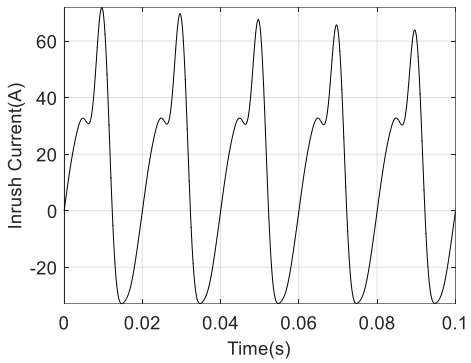

Fig. 11. Transformer Inrush current with zero residual flux and CT saturation at switching angle 0°

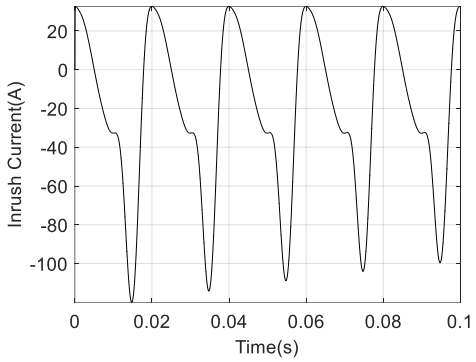

Fig. 12. Transformer Inrush current with 20% residual flux and CT saturation at switching angle 0°

Table.8. The estimation error standard deviation (EESD) of the second studied transformer in the faulty condition, the percentage of changes in EESD with 5% change in the transformer resistance and leakage inductance values, and10% change to the noise matrices values

Location of the fault (%) in the winding	EESD	5% change in the resistance and leakage inductance values	The percentage of changes (%) in EESD	10% change to the noise matrices values	The percentage of changes (%) in EESD
Upper 10%	1.85	1.87	1.08	1.85	0
10 to 20	1.34	1.35	0.75	1.34	0
20 to 30	0.91	0.92	1.09	0.90	1.09
30 to 40	0.64	0.65	1.56	0.64	0
40 to 50	0.42	0.43	2.3	0.43	2.38
50 to 60	0.32	0.32	0	0.32	0
60 to 70	0.20	0.21	5.0	0.21	0
70 to 80	0.12	0.12	0	0.12	0
80 to 90	0.07	0.07	0	0.07	0

In Table 9, in the faulty condition, index β has been calculated for the second studied transformer. The index β in table 9 shows that the maximum value of this index is 3.8% for the faulty phase with the location of the fault in 90% of the winding. Therefore, the index β values in table 9 are in agreement with the index limits. On the other hand, Table 9 shows the percentage of changes in the index β from its previous values. As it can be seen from Table 9, index β has a very small deviation from the noise and parameter mismatch changes.

Table 9. The index β of the second studied transformer in the faulty condition, the percentage of changes in index β with 5% change in the transformer resistance and leakage inductance vales, and10% change to the noise matrices values

Location of the fault (%) in the winding	Index β(%)	5% change the resistance and leakage inductance values	The percentage of changes (%) in Index β	10% change to the noise matrices values	The percentage of changes (%) in Index β

Upper 10%	0.47	0.47	0	0.47	0
10 to 20	0.51	0.51	0	0.51	0
20 to 30	0.58	0.58	0	0.58	0
30 to 40	0.68	0.68	0	.68	0
40 to 50	0.86	0.87	1.16	0.86	0
50 to 60	1.08	1.10	1.85	1.09	0.92
60 to 70	1.44	1.47	2.04	1.46	1.37
70 to 80	1.95	1.98	1.53	1.96	0.51
80 to 90	3.8	3.88	2.10	3.83	0.79

The recognition time of inrush current from fault current, and fault location in the transformer has been shown in Table 10. Intelligent algorithms studied in the other works and customary fault location methods have been compared with the proposed detection time. On the other hand, references [16] and [17] have not given the fault location in the transformer. Table 10 shows that the proposed algorithm has a sensibly well detection time compared to the other methods in fault location and differentiating inrush current from fault current. Besides, the residual signal which is the difference between the estimated and measured currents in case of energizing a faulty transformer has been considered in Table 10. Therefore the absolute residual signal (ARS) using the proposed technique has been compared with the other algorithms in Table 10. Therefore, Table 10 shows that the proposed algorithm has a reasonably well residual signal compared to the other methods in discriminating inrush current from fault current.

Table 10 Localization speed, detection time, and ARS of inrush current from fault current using different algorithms

Algorithm	Mean detection time (ms)	ARS (A)
Proposed	9	5
Wavelet Transform [11]	72	12
Convolutional Neural Network[15]	34	---
[16]	115	14
EKF [17]	5	7
Hermite transform [20]	26	10
Decision Tree [31]	3	---
Artificial Neural Network [31]	487.5	---

Besides, the other algorithms such as wavelet transform require higher sampling rate and are extremely sensitive to noise and unpredicted disturbances. The EKF-based methods have very good robustness since they deal with the measurement and process noises suitably, unlike the wavelet transform that is highly affected by noise and disturbances.

c) The practical implementation and limitations of the proposed method

The electrical fault detection and real-time monitoring system integrates multi microcontroller architecture, real-time sensor monitoring (voltage and current), wireless communication , and cloud-based data logging to create a comprehensive power fault management solution. The system must simulate a miniaturized power distribution network with capabilities to detect Line-to-Ground (L–G) faults, measure real-time electrical parameters, automatically isolate faulty sections using relay-based switching, and provide multi-platform monitoring through OLED displays and web-based dashboards. When a fault is detected, the system sends an SMS to the maintenance personnel notifying them of the type of fault and where it is. This is a real-time alert system that reduces downtimes and allows the services to be restored faster.

The convergence of the extended Kalman filter is locally for nonlinear systems. If the initial estimation error is not too large then as time goes to infinity, the error goes to zero exponentially. In this paper, the convergence of this filter is strongly dependent on the nonlinear characteristic of the core and operating point for fault recognition. Divergence probability of the filter increases if the amplitude of the inrush current is large. Therefore, the probability of divergence is high in power transformers with large changes in core nonlinear characteristic and with large magnitude in inrush current. Besides, the EKF convergence is dependent to the amount of the residual flux. Even by reduction of the time step, convergence is not obtained in these cases. As a result, it is unimaginable that the extended Kalman filter can converge for all values of the switching angle or residual fluxes.

VI. Conclusion

To differentiate between the fault current and the inrush current in a transformer, EKF can be used. The EKF has resistance against measurement noises, the high estimation speed and as well as appropriate estimation accuracy. In this paper, the nonlinear Kalman filter or EKF is used to more accurately estimate the transformer inrush current. The simulated results are presented in different percentages of the winding to the ground fault and is determined the location of the fault. On the other hand, to obtain the estimation error in the steady state, the standard deviation index is also introduced so that to provide an intuitive view of the estimation error. Then again, it is shown that in a faulty transformer, there is always a significant difference between the estimated and the measured inrush current relative to the location of the fault. In addition, an index β is defined for any phase of the transformer so that if the value of this index is in a specific range of value, the location of the fault at the winding can be shown. Thus, it is possible to classify the location of this type of fault in the transformer. Finally, the

proposed technique is implemented for another transformer to calculate the estimation error standard deviation and index β in the faulty condition.

REFERENCES

[1] IEEE Standard C37.91-2000, "IEEE Guide for Protective Relay Applications to Power Transformers", pp.1-85, 9 Oct. 2000, doi: 10.1109/ieeestd.1967.7394911.

[2] H. Yun, Y. Zhang, Y. Sun, L. Wang, L. Xu, D. Zhang, J. Cheng, "Transformer Winding Fault Locating Using Frequency Domain Reflectometry (FDR) Technology" *Electronics*, Vol. 14, No. 15, 3117, 2025, doi:10.3390/electronics14153117

[3] X.Zheng, R. Xian, L.Wang, L.Chen, Y. Hu, H. Hao, G. Liu, "Online Identification Method for Inter-Turn Short-Circuit Fault of Grounding Transformer Winding and Phase Distinction", Measurement, Vol. 256, Part D, 118367, 2025, doi: 10.1016/j.measurement.2025.118367.

[4] H. Dashti, M. Davarpanah, M. Sanaye-Pasand, H. Lesani, "Discrimination Transformer Large Inrush Currents from Fault Currents", International Journal of Electrical Power and Energy Systems, Vol. 75, pp. 74-82, 2016, doi: 10.1016/j.ijepes.2015.08.025.

[5] L. Sun, M. Xu, H. Ren, S. Hu, G. Feng, " Multi-Point Grounding Fault Diagnosis and Temperature Field Coupling Analysis of Oil-Immersed Transformer Core based on Finite Element Simulation", Case Studies in Thermal Engineering, Vol. 55, 104108, 2024, doi: 10.1016/j.csite.2024.104108.

[6] C. Liu, L. Ji, "Transformer Fault Diagnosis Based on Parallel AdaBoost-NB Algorithm on Spark Cloud Platform", International Journal of Grid and High Performance Computing, Vol. 17, No. 1, 2025, doi: 10.4018/IJGHPC.381295.

[7] J. Nosratian Ahour, S. Seyedtabaii, G. B. Gharehepetian, "Determination and Localization of Turn-to-turn Fault in Transformer Winding Using Frequency Response Analysis", IET Science, Measurement and Technology, Vol. 12, No. 3, pp. 291-300, 2018.

[8] A. Torkaman, V. Naeini, "Recognition and Location of Power Transformer Turn to Turn Fault by Analysis of Winding Imposed Forces", Journal of Operation and Automation in Power Engineering, Vol. 7, No. 2, pp. 227-234, 2019, doi: 10.22098/joape.2019.5735.1428.

[9] S. Mulani, S. Y. Gadgune, "Flux Based Technique to Identify the Location of Inter Turn Faults in Transformer", Asian Journal of Convergence in Technology, Vol. 5, No. 3, pp. 87-90, 2020.

[10] S. R. Pani, P. K. Bera, V. Kumar, "Detection and Classification of Internal Faults in Power Transformers using Tree based Classifiers", 2020 IEEE International Conference on Power Electronics, Drives and Energy Systems (PEDES), Jaipur, India, 2020, pp. 1-6, doi: 10.1109/PEDES49360.2020.9379641.

[11] P. Chiradeja, A. Ngaopitakkul, "Winding-to-Ground Fault Location in Power Transformer Windings Using Combination of Discrete Wavelet Transform and Back-Propagation Neural Network", Scientific Reports, Vol. 12, Article number 20157, 2022.

[12] J. P. Américo, J. Vianei Leite, C. Franzoi Mazzola, "A New Model for Inrush Current in Three-Phase Transformers", IEEE Access, Vol. 14, pp. 2001-2014, 2026, doi: 10.1109/ACCESS.2025.3649642.

[13] Z. Babaei, M. Moradi, "Novel Method for Discrimination of Transformers Faults from Magnetizing Inrush Currents Using Wavelet Transform", Iranian Journal of Science and Technology, Transactions of Electrical Engineering, Vol. 45, pp. 803–813, 2021, doi: 10.1007/s40998-020-00399-1.

[14] R. Afsharisefat, M. Jannati, M. Shams, "Discrimination of Inrush Current and Internal Faults Incorporating the MRA and BIGRU Techniques in Power Transformers", Electric Power Systems Research, Vol. 219, Article Number 109255, 2023, doi: 10.1016/j.epsr.2023.109255.

[15] A.A. Athamneh, A.M. Alqudah, "Transformer Inrush Current and Internal Fault Discrimination using Multi-types of Convolutional Neural Network Techniques", Journal of Electrical and Computer Engineering, Vol. 2024, Article Number 3986400, 2024, doi:10.1155/2024/3986400.

[16] S. K. Gunda, V.S.S.S.S. Dhanikonda, "Discimination of Transformer Inrush Currents and Internal Fault Currents Using Extended Kalman Filter Algorithm (EKF)," Energies, Vol. 14, No. 19, 2021, doi: 10.3390/en14196020.

[17] F. Naseri, Z. Kazemi, M. M. Arefi, E. Farjah, "Fast discrimination of transformer magnetizing current from internal faults: an extended Kalman filter-based approach", IEEE Transactions on Power Delivery, Vol. 33, No. 1, pp. 110-118, 2018, doi: 10.1109/TPWRD.2017.2695568.

[18] M. Tajdinian, M. Allahbakhshi, A. Bagheri, H. Samet, P. Dehghanian, O. P. Malik, "An enhanced sub-cycle statistical algorithm for inrush and fault currents classification in differential protection schemes", International Journal of Electrical Power & Energy Systems, Vol. 119, Article Number 105939, 2020, doi: 10.1016/j.ijepes.2020.105939.

[19] R. Dashti, A. Khoshkhoo, H. R. Parish, H. R. Shaker, "A new operational characteristic for diagnosing the healthy and faulty currents of power transformers", Electric Power Systems Research, Vol. 203, Article Number 107649, 2022, doi: 10.1016/j.epsr.2021.107649.

[20] D. Guillen, J. Olveres, H. Esponda, B. Escalante-Ramirez, V. Torres-García, R. Tapia-Olvera, "Hermite transform-based algorithm to discriminate magnetizing currents in transformers", Sustainable Energy, Grids and Networks, Vol. 27, Article Number 100493, 2021, doi: 10.1016/j.segan.2021.100493.

[21] D. Guillen, J.C. Olivares-Galvan, R. Escarela-Perez, D. Granados-Lieberman, E. Barocio, "Diagnosis of interturn faults of single-distribution transformers under controlled conditions during energization", Measurement, Vol. 141, pp. 24-36, 2019, doi: 10.1016/j.measurement.2019.03.044.

[22] A. Lu, T. Ji, Z. Xu, X. Zheng, "Inrush current identification based on mathematical morphology and LSSVM", 2024 9th Asia Conference on Power and Electrical Engineering (ACPEE), Shanghai, China, pp. 1195-1199, 2024, doi: 10.1109/ACPEE60788.2024.10532480.

[23] M. Oztekin, S. Karagol, O. Ozgonenel, "Transformer differential protection with wavelet transform and difference function", Engineering Science and Technology, an International Journal, Vol. 70, Article Number 102144, 2025, doi: 10.1016/j.jestch.2025.102144.

[24] X. Zhao, G. Wu, D. Yang, G. Xu, Y. Xing, C. Yao, A. Abu-Siada, "Enhanced detection of power transformer winding faults through 3D FRA signatures and image processing techniques", Electric Power Systems Research, Vol. 242, Article Number 111433, 2025, doi: 10.1016/j.epsr.2025.111433.

[25] H. Shadfar, H. R. Izadfar, "Frequency response analysis: An overview of the measurement process and interpretation

of results for fault diagnosis and location in power transformers", International Journal of Industrial Electronics Control and Optimization, Vol. 8, No. 2, pp. 149-163, 2025, doi: 10.22111/ieco.2024.49470.1603.

[26] A. Tokic, V. Milardic, I. Uglesic, A. Jukan, "Simulation of three-phase transformer inrush currents by using backward and numerical differentiation formulae", Electric Power Systems Research, Vol. 127, pp. 177–185, 2015, doi: 10.1016/j.epsr.2015.05.020.

[27] M. A. Taghikhani, A. Sheikholeslami, Z. T aghikhani, "Harmonic Modeling of Inrush Current in Core Type Power Transformers using Hartley Transform", Iranian Journal of Electrical and Electronic Engineering, Vol. 11, No. 2, pp. 174-183, 2015, doi: 10.22068/IJEEE.11.2.174.

[28] M.A. Taghikhani, Z. Taghikhani, "Comparison of Hartley and Fourier Transforms in Harmonic Modelling of Five-Limb Core Transformer Inrush Current", IETE Journal of research, Vol. 62, No. 6, pp. 745-751, 2016, doi: 10.1080/03772063.2016.1162675.

[29] D. Simon, "Optimal State Estimation: Kalman, H_∞ and Nonlinear Approaches", John Wiley & Sons, Inc., New Jersey, 2006, doi: 10.1002/ 0470045345.

[30] M. Samami, H. Yaghobi and M. Niaz azari, "Modeling and Simulation of a Transformer with Inter-Turn Fault Including Saturation Effect and Variable Fault Parameters", Iranian Journal of Electrical and Electronic Engineering, Vol. 13, No. 2, pp.170-182, 2017, doi: 10.22068/IJEEE.13.2.170.

[31] S. Rao, S.A.Abbas Kazmi, M.Z. Iftikhar, T.A.H. Alghamdi, M. Alenezi, "Enhancing fault detection and classification in distribution transformers using non-contact magnetic measurements: A comparative study of tree models and neural networks", Energy Reports, Vol. 13, pp. 3469-3488, 2025, doi: 10.1016/j.egyr.2025.03.011.

Appendix A

Mohammad Ali Taghikhani was born in Tehran, Iran. He received the B.Sc. and M.Sc. degrees in electrical engineering from Amirkabir University of Technology, Tehran, Iran, in 1997 and 2000, respectively and received the Ph.D. degree in electrical engineering from Iran University of Science and Technology, Tehran, Iran, in 2008. He is currently an associate professor in the department of engineering, Imam Khomeini International University, Qazvin, Iran. His interests are power transformers, electrical machines, numerical analysis, finite element method, heat transfer and fluid mechanics.